Journal of Alloys and Compounds 480 (2009) 658–661

Contents lists available at ScienceDirect

Journal of Alloys and Compounds

journal homepage: www.elsevier.com/locate/jallcom

Effects of polydispersity index and molecular weight on crystallization kinetics of syndiotactic polystyrene (sPS)

Chen-Ming Chen [a], Tsung-Eong Hsieh [a,*], Ming-Yih Ju [b]

[a] Department of Materials Science and Engineering, National Chiao-Tung University, Hsinchu 30010, Taiwan, ROC
[b] Material and Chemical Research Laboratories, Industrial Technology Research Institute, Hsinchu 30043, Taiwan, ROC

ARTICLE INFO

Article history:
Received 15 December 2008
Received in revised form 25 January 2009
Accepted 1 February 2009
Available online 10 February 2009

Keywords:
Polymers
Elastomers and plastics
Crystal growth
Kinetics

ABSTRACT

Isothermal crystallization kinetics of syndiotactic polystyrene (sPS) is reported in this work with Avrami analytical method. It was found that the spherulite growth rate and overall crystallization rate depend on the crystallization temperatures, average molecular weight ($\bar{M}_W$) and polydispersity index (PDI). The experimental results for the melt and cold crystallization processes of sPS revealed that the PDI and $\bar{M}_W$ exhibit pivotal effects on the crystallization rate, which increases with the decrease of $\bar{M}_W$ and PDI.

1. Introduction

Syndiotactic polystyrene (sPS) possesses a very complicated polymorphic behavior. In the past, structure studies were carried out with X-ray diffraction (XRD), Raman spectroscopy, Fourier transform infrared spectroscopy (FTIR), solid state nuclear magnetic resonance (NMR) and electron diffraction [1]. Four different crystalline forms of sPS have been described so far and termed as α, β, γ and δ. Normally, α and β forms are obtained with the melt process of sPS. The α and β forms are more common and associated with polymer chains in a transplanar conformation while the γ and δ forms are with polymer chains in a helical conformation. For the melt process of sPS, the combination of both α and β forms is obtained, but formation of the β form is proposed to be more favored than that of the α form in the sPS compression molding under pressure. The β form is also favored if sPS is prepared by solvent casting at high temperatures to form the melt of crystallization.

Furthermore, some researchers reported that crystalline forms of sPS could be manipulated with the experimental parameters (e.g. cooling rate, solvents, etc.). Corradini et al. [2] and De Rosa et al. [3] found that different functionality for α and β forms of sPS could be generated with the change of cooling rate. Vittoria et al. [4] explored that some kinds of solvents such as dichloromethane, chloroform, and cyclohexane induced new crystalline forms in fibers, modifying the initial zig-zag planar structure of the chain into helical structure without destroying the orientation of fibers. The same solvent was also utilized to produce the crystallization in glassy sPS [5–7]. Greis et al. [8] completed the structure characterization, reporting that three sPS macromolecules from clusters have two types of handedness. These clusters, which depended on the crystallization rate, could arrange in well-pronounced superstructure and the morphology was also maneuvered with the crystallization condition. Although many polymorphic behaviors of sPS have been studied, fewer literatures on the experimental and theoretical results related to crystallization kinetics are reported.

In this paper, we perform the characterization of melt-crystallized sPS and analyze its kinetics of crystallization and melting behaviors at different weight-average molecular weights ($\bar{M}_W$) and polydispersity index (PDI) with the assistance of Avrami analytical method.

2. Experimental

The commercial sPS used in this study was obtained from Dow Chemicals and purified with extraction of methyl ethyl ketone (MEK). The other sPS samples (i.e. sample I, sample II, sample III, and sample IV) were synthesized by anionic polymerization with metallocene and toluene as catalyst and solvent, respectively. These samples exhibit diverse $\bar{M}_W$ and PDI as listed in Table 1. A differential scanning calorimeter (Perkin-Elmer DSC-7) was utilized for various thermal treatments (quenching, annealing or melt-crystallizing) of the samples and for observation of the melting endothermic peaks. The temperatures and enthalpies were calibrated with high purity indium (In) and tin (Sn) standards. Melting peaks were determined by a scanning rate of 10 °C/min from ambient temperature. During thermal treatments of samples, the fastest programmed cooling water was used for quenching the samples. The crystallization temperature (T_c), glass transform temperature (T_g), melting temperature (T_m), heat release upon temperature (ΔH_c),

* Corresponding author. Tel.: +886 3 5712121x55306; fax: +886 3 5724727.
E-mail address: tehsieh@cc.nctu.edu.tw (T.-E. Hsieh).

0925-8388/$ – see front matter © 2009 Elsevier B.V. All rights reserved.
doi:10.1016/j.jallcom.2009.02.003

Table 1
The thermal properties, $\bar{M}_W$, and PDI of sPS samples.

Sample	T_g (°C)	T_c (°C)	T_m (°C)	ΔH_m (J/g)	$\bar{M}_W$ ($\times 10^4$)	$\bar{M}_W/\bar{M}_n$ (PDI)
Commercial sPS	86.4	125.0	265.5	25.30	10.9	1.78
I	94.0	141.1	270.1	19.40	8.6	3.6
II	90.1	144.3	268.4	27.16	22.0	6.2
III	87.9	144.9	268.9	31.81	20.1	6.1
IV	88.3	146.1	268.9	24.60	16.1	6.0

and heat absorbed during melting (ΔH_m) were determined after sample quenching.

3. Results and discussion

3.1. Characterization of melt-crystallized samples

To better understand the temperature range on isothermal crystallization, kinetic studies were performed [9]. Table 1 shows the thermal properties and molecular weight data of sPS samples.

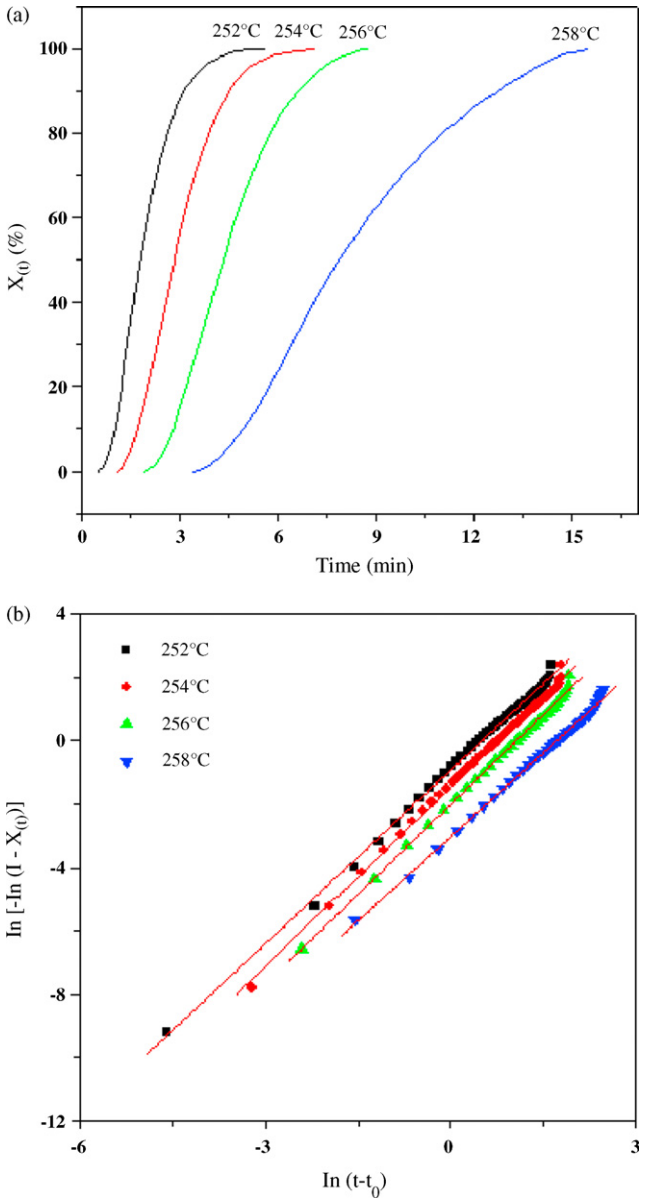

Fig. 1. (a) Crystallization isotherms of sample I at different temperatures and (b) Avrami plot deduced from (a).

We find that the commercial sPS possesses lower T_g, T_c, and T_m than other samples because it may contain atactic PS (aPS), which exhibits less regioregularity than sPS, therefore diminishing the thermal stability.

3.2. Crystallization kinetics

Krzstowczyk et al. [10] have investigated crystallization kinetics of sPS and thus we use Avrami equation to analyze the crystallization kinetic of sPS. Bruce et al. [11] suggested the relative crystallization, $X(t)$, which in semicrystalline polymer may be expressed as

$$X(t) = \frac{m_c}{m} = \exp[-\kappa(t - t_0)^n] \quad (1)$$

where $X(t)$ is the reduced degree of crystallinity, m_c is the weight of crystallinity for the polymer, m is the whole weight for the polymer, κ is the overall crystallization rate constant, n is the Avrami constant and t_0 is the induction time.

Eq. (1) can also be expressed as

$$\ln[-\ln(1 - X(t))] = \ln\ \kappa + n\ln(t - t_0) \quad (2)$$

and

$$\kappa_{1/2} = \frac{\ln 2}{t_{1/2}^n} \quad (3)$$

where $t_{1/2}$ is the time when $X(t) = 1/2$.

The DSC equipped with a mechanical intracooler was utilized for determining the reduced degree of crystallization and times. Typical crystallization isotherms obtained by plotting reduced crystallization *versus* time are shown in Fig. 1(a) for the sample I when crystallized from the melt state. From these curves, the half time of crystallization ($t_{1/2}$) defined as the time required for half of the final crystallization to develop is obtained. The bulk kinetics of crystallization for sPS is analyzed with Eq. (2). Both κ and n depend on the nucleation and growth mechanisms of the crystals. The experimental data fit the Avrami equation well, as for any temperature of $\ln[-\ln(1 - x(t))]$ *versus* $\ln(t - t_0)$ are linear for

Table 2
The crystallization kinetics data of sPS samples when crystallized from the glass state.

Sample	Temperature (°C)	n	κ (t^{-n})	$t_{1/2}$ (min)
Commercial sPS	110	1.3	0.90	0.867
	120	1.3	2.11	0.418
	125	1.5	4.58	0.261
	130	1.7	17.97	0.137
	135	1.4	26.72	0.064
I	130	1.9	1.82	0.655
	135	1.7	2.97	0.429
	140	1.7	7.31	0.255
	145	1.7	12.61	0.165
	150	1.6	27.03	0.096
II	135	1.5	0.81	0.943
	140	1.5	1.58	0.582
	145	1.6	3.38	0.372
	150	1.5	8.98	0.179
III	130	1.4	0.32	1.959
	135	1.4	0.96	0.858
	140	1.6	2.70	0.401
	145	1.7	9.29	0.212
	150	1.6	18.11	0.141
	155	1.8	42.20	0.099
IV	130	1.3	0.95	0.757
	135	1.1	2.37	0.296
	143	1.5	7.51	0.211
	150	1.7	19.77	0.130

Table 3
The crystallization kinetics data of sPS sample when crystallized from the melt state.

Sample	Temperature (°C)	n	$\kappa \times 10^2$ (t^{-n})	$t_{1/2}$ (min)
Commercial sPS	248	1.8	145.63	0.614
I	252	1.8	39.30	1.289
	254	1.9	23.02	1.754
	256	1.9	13.42	2.394
	258	1.8	4.84	4.463
II	243	2.4	131.3	0.755
	245	2.2	51.8	1.058
	248	2.1	26.6	1.554
	250	2.0	13.2	2.248
	253	2.0	4.7	3.866
III	245	2.0	72.7	0.853
	248	2.2	21.3	1.495
	250	2.0	18.4	1.775
	253	2.2	5.8	2.966
	255	2.1	3.7	4.136
IV	245	2.1	151.0	0.714
	248	2.4	70.2	0.981
	250	2.4	26.4	1.453
	253	2.3	7.5	2.617
	255	2.2	3.7	3.794

long crystallization time (see Fig. 1(b)) and we can acquire n and κ since the slope and intercept are n and $\ln \kappa$, respectively. Moreover, Fig. 1(b) also indicates that the secondary crystallization can be excluded. By the same method, the kinetic crystallization data of other samples were obtained and listed in Tables 2 and 3.

The variation of $t_{1/2}$ with temperatures for the samples crystallized from the glass and melt states are shown in Figs. 2 and 3, respectively. In case of crystallization from glass states, $t_{1/2}$ decreases with the increase of the temperature. In case of crystallization from melt states, however, $t_{1/2}$ rises with the raise of the temperature. Figs. 4 and 5 show the overall crystallization rate constant (κ) as a function of temperature for the samples crystallized from the glass and melt states. The experimental results reveal that κ increases with the rise of the temperature when crystallized from the glass state but drops with the raise of the temperature when crystallized from the melt state.

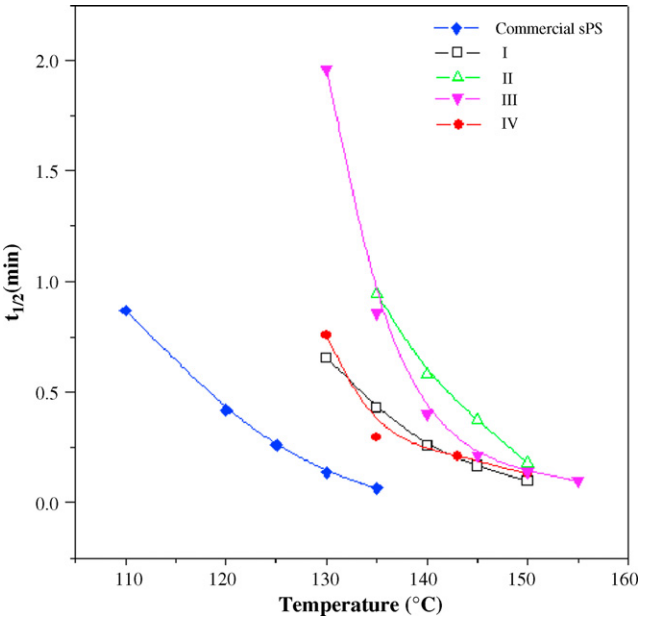

Fig. 2. The variation of $t_{1/2}$ of sPS with temperature when crystallized from the glass state.

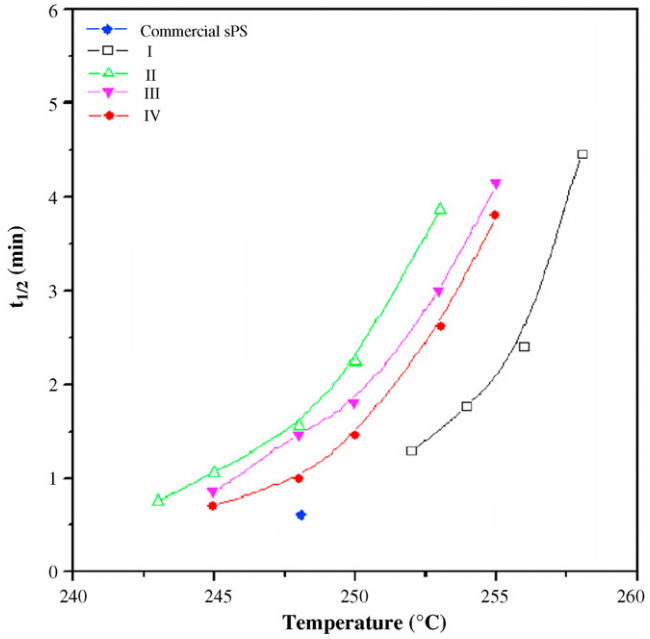

Fig. 3. The variation of $t_{1/2}$ of sPS with temperature when crystallized from the melt state.

As shown in Figs. 2–5, the commercial sPS exhibits a higher crystallization rate than other samples when crystallized from both the glass and melt states. This is attributed to the doping of aPS in the commercial sPS. When aPS melts with sPS, the crystallization rate of sPS subsequently increases. Hong et al. [12] found that the spherulite growth rate and overall crystallization rate of sPS in blends enhanced with the increasing amount of aPS, representing that sPS is miscible with aPS. In general, the spherulite growth rate of crystallizable polymer, at a given T_c, depends on the energetic terms, e.g. the activation free energy required for the transport process through the liquid–solid interface and the free energy for the formation of nucleus size. The raise in spherulite growth rate of sPS/aPS blends is due to an increase of nucleus size that may

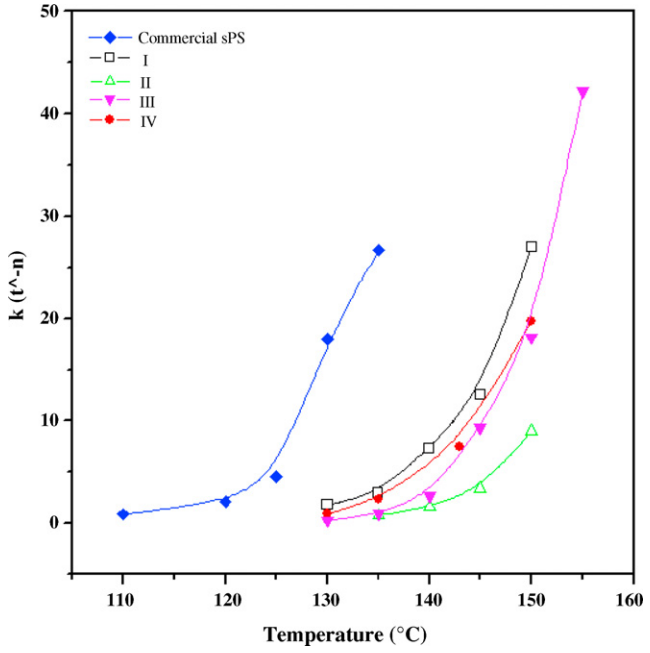

Fig. 4. The overall crystallization rate constant as a function of temperature for the sPS samples when crystallized from the glass state.

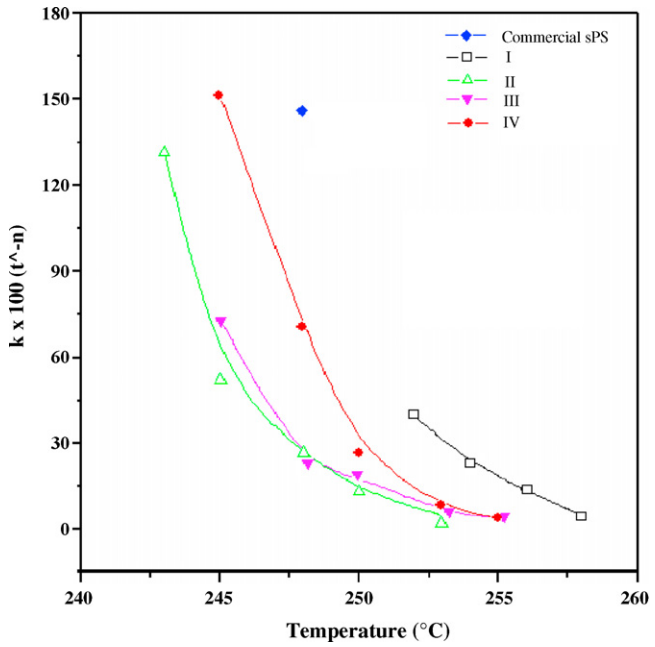

Fig. 5. The overall crystallization rate constant as a function of temperature for the sPS samples when crystallized from the melt state.

rise from a dilution effect associated with a plenty concentration of crystallizable components at the crystal growth front.

We also found that the PDI and $\bar{M}_W$ are crucial factors for the crystallization of sPS from the glass and melt states. As manifested in Figs. 2–5, the crystallization rate increases with the decrease of PDI when crystallized from both the glass and melt states. The sPS samples with high PDI ($\bar{M}_W/\bar{M}_n$) mean they have small molecules since they exhibit small $\bar{M}_n$ based on the same $\bar{M}_W$. The small molecules play a diluent role in the sPS samples, inhibiting the grain growth. The reason is that small molecules have small thermal driving force, restricting the grain growth [10]. From this reason, the commercial sPS with small PDI exhibits the higher crystallization rate both from glass and melt states. In addition, we also observed that the crystallization rate rises with the drop of $\bar{M}_W$ when crystallized from both the glass and melt states. The high $\bar{M}_W$ of sPS induces a high viscosity, amplifying the difficulty for the diffusion of the chains to the crystallization sites and therefore slowing down the crystallization rate. At high temperatures, the rate-limiting step is no longer diffusion, but switches to the thermodynamically controlled crystallization [12].

4. Conclusions

This work presents the crystallization kinetics of sPS at different temperatures with Avrami analytical method. It was found that the crystallization rate of sPS doping with aPS can be accelerated and that of pure sPS increases with the decrease of PDI and $\bar{M}_W$ when crystallized from both the glass and melt states.

Acknowledgement

This work is supported by National Science Council (NSC), Taiwan, R.O.C., under contract No. NSC93-2216-E-009-008.

References

[1] R.H. Lin, E.M. Woo, Polymer 41 (2000) 121.
[2] P. Corradini, C. De Rosa, G. Guerra, R. Napolitano, V. Petraccone, B. Pirozzi, Eur. Polym. J. 30 (1994) 1173.
[3] C. De Rosa, M. Rapacciuolo, G. Guerra, V. Petraccone, P. Corradini, Polymer 33 (1992) 1423.
[4] V. Vittoria, R. Russo, F. de Candia, Polymer 32 (1991) 3371.
[5] C. Rober, L. Curt, Polymer 36 (1995) 2331.
[6] F.D. Candia, M. Carotenuto, L. Guadagno, V. Vittoria, J. Macromol. Sci.-Phys. B35 (1996) 265.
[7] M. Tosaka, N. Hamada, M. Tsuji, S. Kohjiya, T. Ogawa, S. Isoda, T. Kobayashi, Macromolecules 30 (1997) 4132.
[8] O. Greis, Y. Xu, T. Asano, J. Petermann, Polymer 30 (1989) 590.
[9] E.B. Orler, J. Dorie, R.B. Moore, Macromolecules 26 (1993) 5157.
[10] D.H. Krzstowczyk, X. Niu, R.D. Wesson, J.R. Collier, Polym. Bull. 33 (1994) 109.
[11] E.B. Bruce, R.B. Moore, Polym. Prepr. 35 (1994) 423.
[12] B.K. Hong, W.H. Jo, J. Kim, Polymer 39 (1998) 3753.